

Russian Nesting Doll Complexes of Molecular Baskets and Zinc Containing TPA Ligands

Lei Zhiquan, Shane Polen, Christopher M. Hadad, T. V. RajanBabu, and Jovica D. Badjić*

Department of Chemistry and Biochemistry, The Ohio State University, 100 West 18th Avenue, Columbus, Ohio 43210, United States

Supporting Information

ABSTRACT: In this study, we examined the structural and electronic complementarities of convex 1–Zn(II), comprising functionalized tris(2-pyridylmethyl)amine (TPA) ligand, and concave baskets 2 and 3, having glycine and (S)-alanine amino acids at the rim. With the assistance of ¹H NMR spectroscopy and mass spectrometry, we found that basket 2 would entrap 1–Zn(II) in water to give equimolar 1–ZnC_{2in} complex ($K = (2.0 \pm 0.2) \times 10^3 \text{ M}^{-1}$) resembling Russian nesting dolls. Moreover, C₃ symmetric and enantiopure basket 3, containing (S)-alanine groups at the rim, was found to transfer its static chirality to entrapped 1–Zn(II) and, via intermolecular ionic contacts, twist the ligand's pyridine rings into a left-handed (M) propeller (circular dichroism spectroscopy). With molecular baskets embodying the second coordination sphere about metal-containing TPAs, the here described findings should be useful for extending the catalytic function and chiral discrimination capability of TPAs.



INTRODUCTION

As a part of the quest toward developing novel methods for chemical functionalization of abundant and inexpensive natural gas,^{1,2} chemists have worked on mimicking the action of copper,^{3,4} and iron⁵ containing monooxygenases.⁶ In essence, studies^{7–10} centered on understanding structural characteristics and catalytic behavior of copper and iron coordination complexes of tris(2-pyridylmethyl)amine (TPA, Figure 1A) have been of great value for developing fundamental knowledge pertaining to the selective activation of strong C–H bonds.¹¹ Que and co-workers have, for instance, found that TPA–Fe(II) catalyzes stereospecific insertion of an oxygen atom from H₂O₂ into C–H bonds of hydrocarbons.¹² Moreover, TPA–Cu(II) complexes promote hydroxylation of substrates by way of forming fleeting copper–oxo intermediates.^{13,14} Copper and zinc complexes of TPAs are also of great value for diagnosing the presence of targeted substances in environment¹⁵ and, in particular, reporting on their stereoisomeric proportion.¹⁶ For instance, one can use Zn(II) or Cu(II) complexes of chiral TPA for rapid determination of enantiomeric excess of alcohols, carboxylic acids, and amines.^{17–20} In this vein, dynamic propeller chirality in TPA ligands has been controlled with an alkyl substituent at the stereogenic benzylic carbon (Figure 1A). The alkyl group acts as a relay auxiliary to, via van der Waals interactions, promote the exclusive formation of right- or left-handed stereoisomer.²¹ In line with the versatile nature of TPA complexes and their potential role in catalysis and recognition, we hereby report on the capacity of C₃ symmetric baskets²² of type 2 to surround 1–Zn(II) in water (Figure 1). Moreover, the chirality in these nesting complexes (resembling Russian matryoshka dolls)^{23,24} is transferred from the chiral and concave basket of the exterior to achiral and convex ligand holding the electrophilic metal cation of the interior. As

molecular baskets embody the second coordination sphere²⁵ around metal-containing TPA,²⁶ we reason that our finding could be useful for enhancing the catalytic function of transition metals²⁷ and extending the scope of chiral discrimination technologies.¹⁶

RESULTS AND DISCUSSION

At first, we aimed to probe structural and electronic complementarity²⁸ of TPAs and amino acid-functionalized baskets²⁹ in polar water solvent (Figure 1A).³⁰ Accordingly, we wondered whether C₃ symmetric 1–Zn(II) with three positively charged ammonium groups at its periphery would complex C_{3v} symmetric basket 2 carrying three negatively charged carboxylates at the rim and give dimeric 1–ZnC_{2out} capsule (Figure 1B) held together by charged hydrogen bonds.^{31–33} These two compounds could also assemble by shielding their hydrophobic surfaces³⁴ in water, thereby giving nesting complex 1–Zn(II)C_{2in} (Figure 1B). To test our hypotheses, we set to prepare guest 1–Zn(II) (Scheme 1) and hosts 2 and 3.

Compound 1 was obtained from commercially available methyl 6-methylnicotinate 4 in seven synthetic steps and overall 24% yield (Scheme 1). In particular, the radical bromination of 4 yielded the corresponding *gem*-dibromide, which upon reduction with diethyl phosphite gave compound 5. This electrophilic molecule was, in the presence of nucleophilic ammonia, and under controlled experimental conditions, subjected to trimerization to give TPA 6.³⁵ The conversion of methyl esters from 6 into hydroxyl groups in 7 was then completed with lithium borohydride. Finally, the

Received: April 29, 2016

Published: June 15, 2016

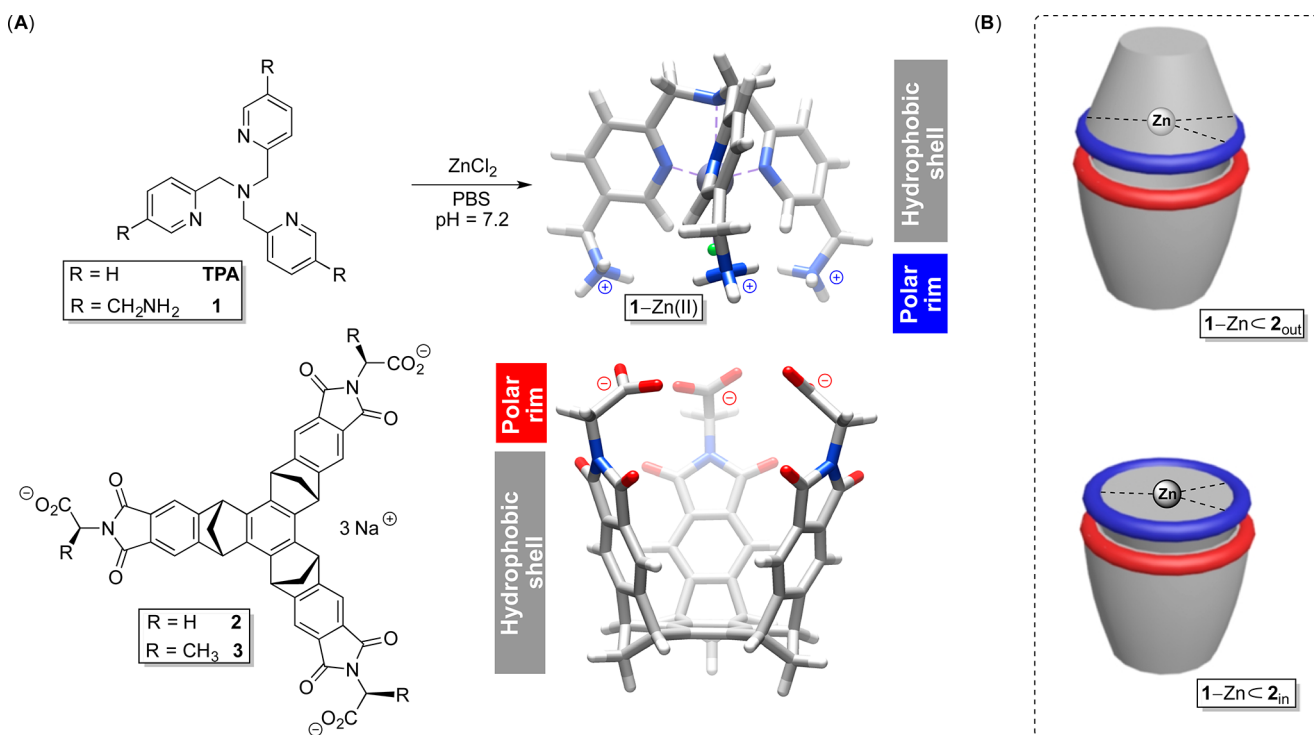
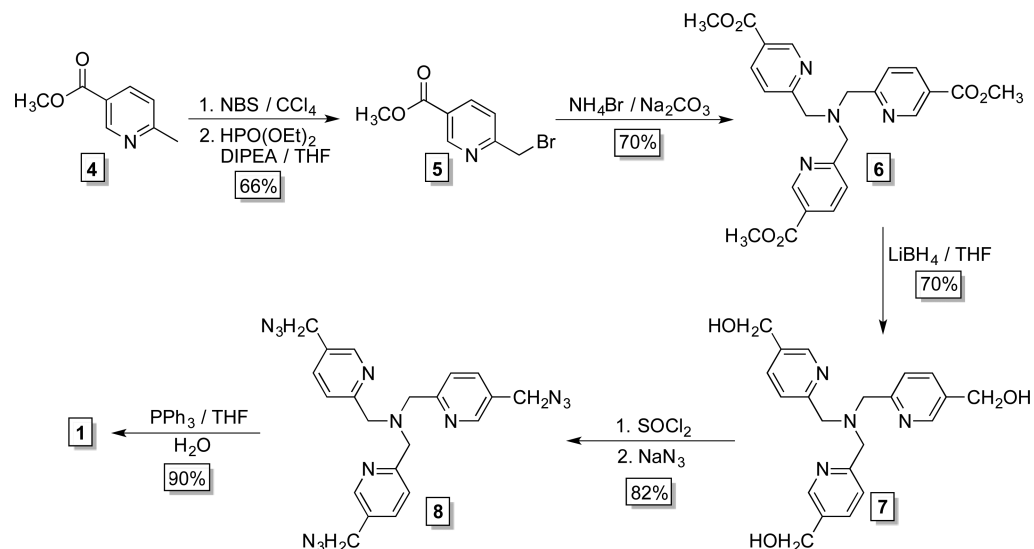


Figure 1. (A) Chemical structures of tris(2-pyridylmethyl)amine (TPA), **1**, and baskets **2** and **3**. Energy-minimized structures (MMFFs, Spartan) of C_3 symmetric **1-Zn(II)** and **2**, showing their electronic and structural complementarity. (B) A schematic representation of two possible ways for the assembly of **1-Zn(II)C₂** in water: capsular **1-Zn(II)C₂_{out}** (top) and nesting **1-Zn(II)C₂_{in}** (bottom).

Scheme 1. Synthetic Method for Obtaining **1**



stepwise conversion of three hydroxyls from **7** into azides in **8** followed by the Staudinger reduction of these functional groups yielded tris-amine **1** (Scheme 1). An incremental addition of $ZnCl_2$ to **1**, in phosphate buffer at $pH = 7.2$, gave stable polydentate **1-Zn(II)** complex (Figure S1; see also Figure 1A).²¹ Baskets **1** and **2**, containing glycine and (S)-alanine residues at the portal, were prepared using previously reported methods.²⁹

¹H NMR spectra (600 MHz, 298 K) of **1-Zn(II)** and **2**, each in 10 mM phosphate buffer at $pH = 7.2$, revealed a set of resonances corresponding to, on average, C_{3v} symmetric molecules (Figure 2A/E). The spectra were assigned with the

assistance of two-dimensional ¹H-¹H NOESY and ¹H-¹³C HMQC cross-correlations (Figure S2). To determine pK_a values of **1** and **1-Zn(II)** in water, we recorded ¹H NMR spectra of these molecules in 10 mM phosphate buffer at $pH = 6-11$ (Figure 2B; see also Figure S3). A change in the chemical shift of H_k proton as a function of pH was sigmoidal with $pK_a = 9.0$ for **1** and 8.9 for **1-Zn(II)**.^{36,37} In line with the result, we chose to complete all of our measurements at $pH = 7.2$, at which three ammonium groups of the multidentate ligand, with and without zinc metal, remain predominantly protonated.

The apparent lack of line broadening of proton signals of **1-Zn(II)** and **2** in water (Figure 2A) suggested the absence of

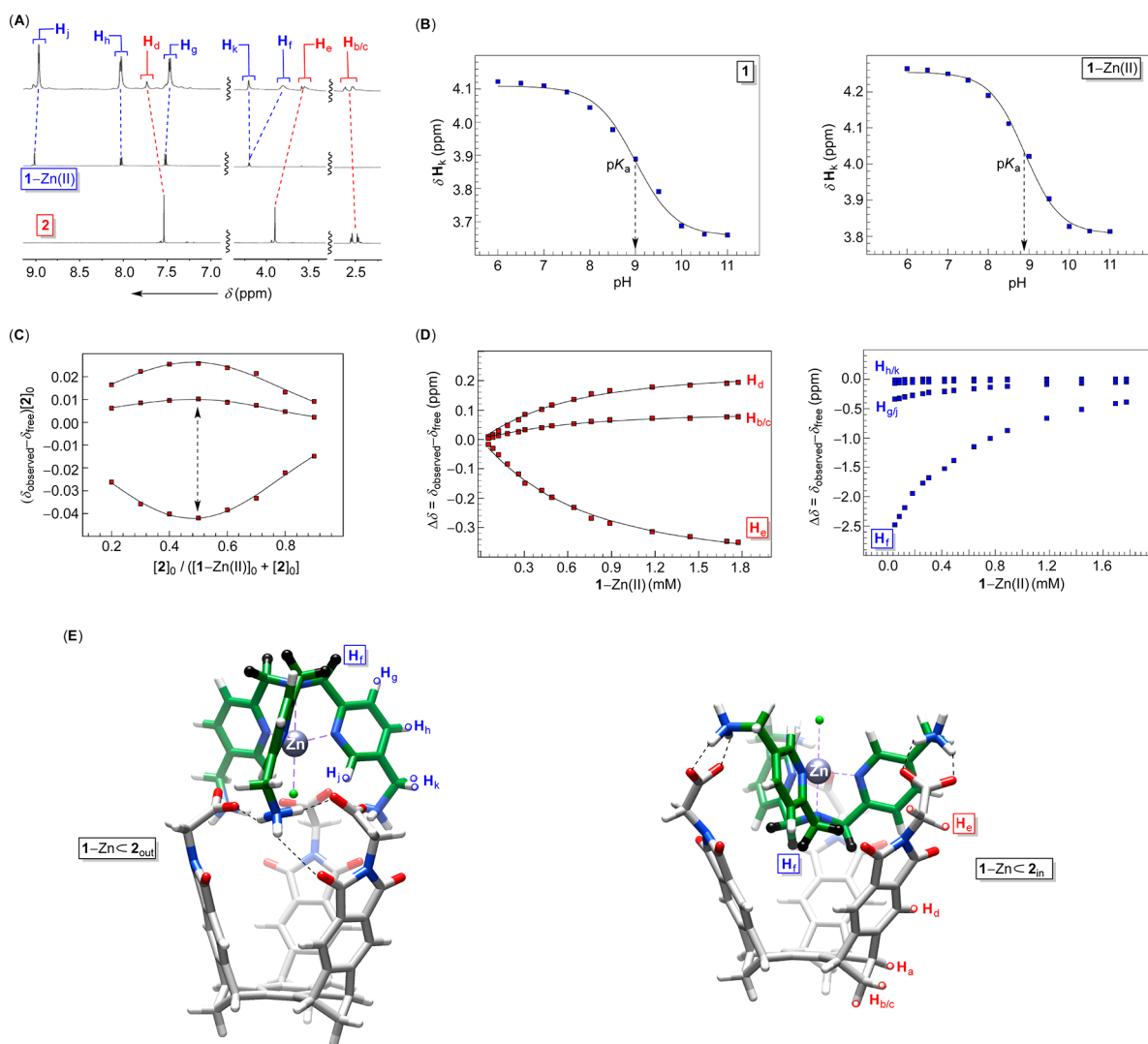


Figure 2. (A) ^1H NMR spectra (600 MHz, 298 K) of basket **2** (0.31 mM, bottom), ligand **1-Zn(II)** (2.0 mM, middle), and their 1:7 mixture (top; for other ratios, see Figure S4) in 10 mM phosphate buffer at pH = 7.2. (B) ^1H NMR chemical shift (600 MHz, 298 K) of singlet corresponding to H_k in **1** (left) and **1-Zn(II)** (right) as a function of pH (10 mM phosphate buffer). The nonlinear least-squares fitting of the experimental data^{36,37} to $\delta_{\text{observed}} = [(\delta_{\text{max}} + (\delta_{\text{min}} - \delta_{\text{max}})10^{(\text{pH}-\text{pK}_a)})]/(1 + 10^{(\text{pH}-\text{pK}_a)})$ gave pK_a values of 8.99 ± 0.06 ($R^2 = 0.99$, top) and 8.90 ± 0.04 ($R^2 = 0.99$, bottom). (C) The Job plot corresponding to the formation of **1-ZnC2** was obtained with ^1H NMR spectroscopy (600 MHz, 298 K) and $[\text{1-Zn(II)}]_0 + [\text{2}]_0 = 0.48$ mM. (D) Chemical shifts of proton nuclei in **1-Zn(II)** (blue) and **2** (red) were obtained upon an incremental addition of a standard solution of the ligand (8.5 mM) to basket (0.31 mM) in 10 mM phosphate buffer at pH = 7.2 (see Figure S4). The nonlinear least-squares fitting of the experimental isotherms from H_{b-e} resonances (red) to a 1:1 stoichiometric model gave the association constant $K = (2.0 \pm 0.2) \times 10^3 \text{ M}^{-1}$ ($R^2 = 0.99$). (E) Energy-minimized structures (PM3, Spartan) of complexes **1-ZnC2_{out}** and **1-ZnC2_{in}** showing structurally nonequivalent proton nuclei.

intermolecular aggregates and/or the formation of dynamic and equilibrating structures.³⁸ Importantly, an incremental addition of a standard solution of **1-Zn(II)** (8.5 mM) to **2** (0.31 mM) led to the perturbation of magnetic environments of all proton nuclei (Figure 2A/D) to indicate the formation of host-guest complexes. In particular, the method of continuous variation³⁹ (the Job plot, Figure 2C) revealed bell-shaped curves peaking at the equimolar host-guest ratio. Indeed, the nonlinear least-squares fitting of ^1H NMR titration data (Figure 2D) to a 1:1 stoichiometric model was satisfactory,⁴⁰ to give the association constant $K = (2.0 \pm 0.2) \times 10^3 \text{ M}^{-1}$. The formation of **1-ZnC2** was finally corroborated with ESI mass spectrometry (Figure S5), in which a peak observed at $m/z = 621.16$ corresponds to doubly charged molecular ion of the complex.

How does multivalent $^1\text{Zn(II)}$ and **2** combine in polar water to give the observed equimolar complex?³⁰ In line with

the original hypotheses (Figure 1B), we completed energy minimizations of **1-ZnC2_{in}** and **1-ZnC2_{out}** in a vacuum (PM3, Spartan)⁴² to find a somewhat greater stability of **1-ZnC2_{out}** ($\Delta\Delta H_{\text{formation}}^\circ = 3.1$ kcal/mol, Figure 2E).^{31,32} While **1-ZnC2_{out}** complex encompasses nine, **1-ZnC2_{in}** contains six N-H...O hydrogen bonds: a greater number of hydrogen bonding contacts could, in part, account for the computed stability of capsular **1-ZnC2_{out}** in a vacuum. As the complexation was probed in polar water solvent, however, the solvation and entropic factors (ΔS°) must also be taken into consideration for evaluating the relative stability (ΔG°) of the two complexes (see below).³⁰

During the formation of **1-ZnC2**, ^1H NMR singlet corresponding to H_f nuclei in **1-Zn(II)** became far more magnetically shielded ($\Delta\delta = 2.5$ ppm, Figure 2D; see also Figure S6) than any other resonance from the guest! The

observation can actually be elucidated by considering the energy-minimized structure of $1\text{-ZnC2}_{\text{in}}$ (Figure 2E): H_f protons are in this complex situated against four aromatic rings of the cup-shaped host and therefore poised to become diamagnetically shielded. In contrast, a negligible magnetic perturbation of H_f is expected for $1\text{-ZnC2}_{\text{out}}$ complex (Figure 2E) encompassing these nuclei at the northern side and far from the basket. The formation of nesting $1\text{-ZnC2}_{\text{in}}$ was also evident from the results of a competition experiment (Figure S7).⁴³ First, we populated the hydrophobic cavity of basket **2** in 10 mM phosphate buffer at pH = 7.2 with iso- C_4H_{10} gas ($K = 93 \text{ M}^{-1}$).⁴⁴ The encapsulation was manifested (^1H NMR spectroscopy) with an upfield chemical shift of the guest's nuclei ($\delta_{\text{observed}} = 0.66 \text{ ppm}$, $\delta_{\text{free}} = 0.76 \text{ ppm}$; Figure S7). Next, we added 1-Zn(II) to $2\text{Ciso-C}_4\text{H}_{10}$ and noted a complete release of the trapped isobutane molecules back into the aqueous solution ($\delta_{\text{observed}} = \delta_{\text{free}} = 0.76 \text{ ppm}$, Figure S7). Apparently, the predominant formation of $1\text{-ZnC2}_{\text{in}}$ prompted the substitution of iso- C_4H_{10} , residing in the basket's cavity, with 1-Zn(II) . Importantly, complex $1\text{-ZnC2}_{\text{out}}$ ($V = 143 \text{ \AA}^3$; Figure 3D)⁴⁵ should be capable of holding a molecule of the

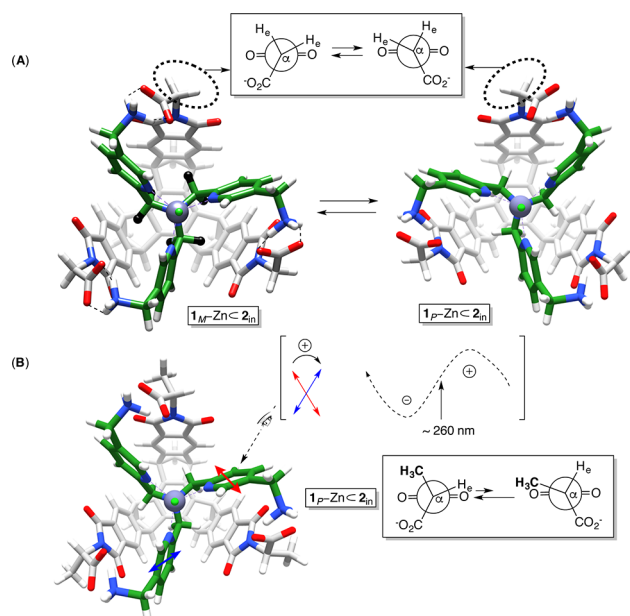


Figure 3. (A) Top view of energy-minimized (PM3, Spartan) structures of $1_{P/M}\text{-ZnC2}_{\text{in}}$ complexes, showing left- (*M*) and right-handed (*P*) sense of twist of the pyridine rings. (B) A chirality transfer from enantiopure basket **3** to ligand 1-Zn(II) (PM3, Spartan) is expected to result in twisting of the pyridine groups into *M*-shaped propeller and the positive coupling of three transition dipole moments (two are shown as red and blue double-headed arrows) at 260 nm.

hydrocarbon ($V = 80 \text{ \AA}^3$, Spartan) in its inner space (PC = 56%),⁴⁶ yet no gas encapsulation was observed due to, we posit, nonexistence or a low concentration of $1\text{-ZnC2}_{\text{out}}$ assembly.

The formation of $1\text{-ZnC2}_{\text{in}}$ was, in our ^1H NMR titration experiment, also characterized with an upfield shift of the resonance corresponding to H_e protons of the host ($\Delta\delta = 0.35 \text{ ppm}$, Figure 2D). To account for the observation, we reasoned that the formation of N-H...N hydrogen bonds should fasten the CH_2CO_2^- groups in the vicinity of the pyridine rings from multidentate 1-Zn(II) (Figure 3A) and thereby place H_e protons in the shielding region of the aromatics.⁴⁷ Moreover, these ionic contacts appear to augment the thermodynamic

stability of $1\text{-ZnC2}_{\text{in}}$. That is to say, the standard free energy (ΔG° , 298 K) for the formation of **1C2**, containing CH_2NH_3^+ groups, is 5.8 kcal/mol (Figure S8), while the stability of **TPAC2**, lacking CH_2NH_3^+ groups, is 4.9 kcal/mol (Figure S9). It follows that the measured difference in thermodynamic stability of $\Delta\Delta G^\circ \approx 1 \text{ kcal/mol}$ should, in large part, emerge from the ionic N-H...N contacts.⁴⁸ The remaining portion of stabilization energy of $\Delta G^\circ \approx 5 \text{ kcal/mol}$ is substantial to suggest that nonpolar contacts and hydrophobic effect⁴⁹ play the central role in the formation of nested complexes. Indeed, the formation of **TPA-2** was in 30 mM phosphate buffer at pH = 7.2 examined with isothermal titration calorimetry (298.0 K, Figure S10) to show a greater entropic contribution ($T\Delta S^\circ = 2.97 \pm 0.11 \text{ kcal/mol}$, $\Delta H^\circ = -1.53 \pm 0.08 \text{ kcal/mol}$) to the free energy of the complexation ($\Delta G^\circ = -4.50 \pm 0.08 \text{ kcal/mol}$).

By forming the ionic contacts, three carboxylates in $1\text{-ZnC2}_{\text{in}}$ assume clockwise and counterclockwise orientations about the basket's rim (Figure 3A). This, in turn, twists the pyridine rings in entrapped 1-Zn(II) to the right (*P*) or to the left (*M*): as basket **2** is achiral, we envisioned the formation of racemic 1-Zn(II) with *P/M* enantiomers in a dynamic equilibrium. Importantly, one $\alpha\text{C-H}_e$ group in energy-minimized $1_{P/M}\text{-ZnC2}_{\text{in}}$ (Figure 3A) is nearly eclipsing the juxtaposed carbonyl functionality. This spatial arrangement is actually known⁴⁴ to prevail in amino acid-functionalized phthalimides possessing an R group larger than hydrogen ($\text{R}\alpha\text{CHPhCO}_2^-$; $\text{R} \neq \text{H}$), while with $\text{R} = \text{H}$ the carboxylate stays perpendicular to the phthalimide ring. In fact, our earlier study⁴⁴ showed that this conformational bias results from (a) van der Waals A^{1-3} type of strain between the juxtaposed $\text{C}=\text{O}$ and CO_2^-/R groups and (b) favorable n-to- σ^* hyperconjugation with the lone pair on the nitrogen acting as a donor and $\alpha\text{C-C}$ bonds of the CO_2^-/R groups accepting the electrons. A question arose: if the $\alpha\text{C-H}_e$ bond in $1\text{-ZnC2}_{\text{in}}$ is indeed eclipsing the phthalimide ring, will basket **3** with (*S*)-alanine groups at its rim (Figure 3B) and $\alpha\text{C-H}_e$ eclipsing the juxtaposed imide⁴⁴ be more preorganized²⁸ than **2** (Figure 1A) for entrapping 1-Zn(II) ? Additionally, the chiral host should transfer its static chirality to trapped 1-Zn(II) (Figure 3B) and, by virtue of three ionic contacts, twist its pyridine groups into *M* propeller to give $1_M\text{-ZnC3}_{\text{in}}$! In this regard, pyridine chromophores are in **TPA-Zn(II)** complexes known¹⁸ to possess an electronic π -to- π^* transition at 260 nm ($^1\text{B}_2$ type), polarized along the direction perpendicular to the N-C₄ axis of the pyridine ring (Figure 3B). In line with the exciton chirality method (ECCD),⁵⁰ there should be an exciton coupling of the $^1\text{B}_2$ transition dipole moments in $1_M\text{-ZnC3}_{\text{in}}$ to give a bisignate spectrum. The sign of this CD couplet is based on the semi empirical rule:⁵¹ the positive chirality (for the longer wavelength component, $\Delta\epsilon > 0$) is obtained when the chromophores are positioned in space so that a clockwise rotation of the front electric dipole moment by an acute angle brings it onto the exciton dipole in the back. On the basis of the rule and the above reasoning, we expected a positive CD couplet for $1_M\text{-ZnC3}_{\text{in}}$ at 260 nm (Figure 3B).

An incremental addition of standard solution of 1-Zn(II) to basket **3** in 10 mM phosphate buffer at pH = 7.2 was followed by ^1H NMR spectroscopy to reveal the formation of equimolar $1\text{-ZnC3}_{\text{in}}$ (Figure S11). As the magnetic perturbation of host's nuclei H_{b-e} in $1\text{-ZnC3}_{\text{in}}$ (Figure 4A) was commensurate with those observed for $1\text{-ZnC2}_{\text{in}}$ (Figure 2D), we concluded that these two assemblies possess similar structural characteristics.

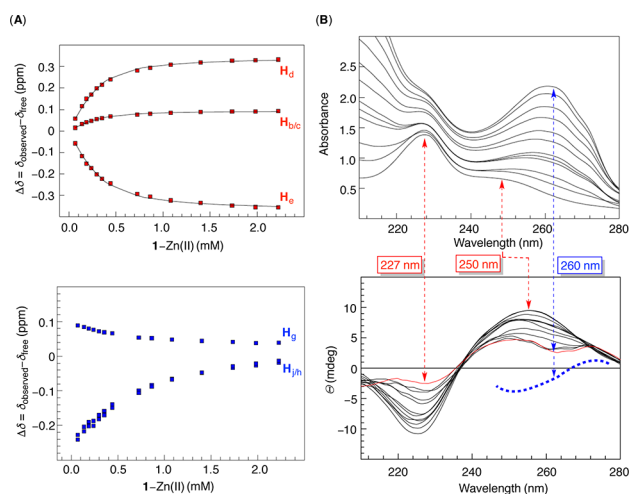


Figure 4. (A) Chemical shifts of proton nuclei in 1-Zn(II) (blue) and 3 (red) were obtained upon an incremental addition of a standard solution of the ligand (20.9 mM) to basket (0.3 mM) in 10 mM phosphate buffer at pH = 7.2 (see also Figure S10). The nonlinear least-squares fitting of the experimental isotherms from H_{b-e} resonances (red) to a 1:1 stoichiometric model gave the association constant $K = (1.0 \pm 0.3) \times 10^4 \text{ M}^{-1}$ ($R^2 = 0.99$); H_e signal corresponds to CH_3 group (Figure S10). (B) A series of UV-vis (top) and circular dichroism (bottom) spectra of basket 3 (13.5 μM) in 10 mM phosphate buffer at pH = 7.2 was obtained upon an incremental addition of 0–12 mol equiv of 1-Zn(II) (1.35 mM); note that the red CD spectrum depicts the end point of the titration.

Importantly, the stability constant corresponding to the formation of 1-ZnC3_{in} ($K = (1.0 \pm 0.3) \times 10^4 \text{ M}^{-1}$, Figure 4A) is an order of magnitude greater than that measured for 1-ZnC2_{in} ($K = (2.0 \pm 0.2) \times 10^3 \text{ M}^{-1}$, Figure 4A). As originally anticipated, basket 3 indeed appears better preorganized, than 2, for forming multiple ionic contacts with 1-Zn(II) and trapping this complex in its inner space! Next, the formation of 1-ZnC3_{in} was monitored with UV-vis and CD spectroscopies. Enantiopure host 3 showed two prominent π -to- π^* electronic transitions originating from its three phthalimide chromophores, one at 227 nm and another at \sim 250 nm (Figure 4B).⁵² These two transitions are also contributing to the Cotton effects observed for the host at 225 and \sim 255 nm. An incremental addition of 1-Zn(II) guest to basket 3 (Figure 4B), however, caused a reduction in the intensity of two bands from the host with the emergence of a positive CD couplet from 1-Zn(II) centered at 260 nm; we reason that the left portion of the couplet is masked with the absorption of circularly polarized light from the host's phthalimides. The observation is thus in line with the *M* disposition of three pyridine chromophores within 1_M-ZnC3_{in}, suggesting that the transfer of chirality is in this supramolecular environment operating in a controllable and predictable manner.

CONCLUSION

We discovered that molecular baskets carrying amino acids at the rim could accommodate metal-containing TPA ligands in their inner space. These nesting assemblies, resembling the Russian stacking dolls, are stable in polar water solvent with their formation primarily driven by desolvation of host/guest nonpolar surfaces. Notably, the enantiopure basket acts as a second coordination sphere to set the axial chirality of the metal containing ligand in its inner space. Given a great value of TPA

coordination compounds for promoting catalytic C–H activations and chiral discriminations, we reason that the here described concept should find its application in the areas of catalysis and molecular recognition. At present, we are investigating the catalytic capability of iron- and copper-based nesting complexes in the activation of small hydrocarbons in water.

ASSOCIATED CONTENT

Supporting Information

The Supporting Information is available free of charge on the ACS Publications website at DOI: 10.1021/jacs.6b04436.

Additional details of the experimental protocols (PDF)

AUTHOR INFORMATION

Corresponding Author

*badjic@chemistry.ohio-state.edu

Notes

The authors declare no competing financial interest.

ACKNOWLEDGMENTS

The experimental portion of this work was financially supported with funds obtained from the U.S. National Science Foundation under CHE-1305179 (to J.D.B.), CHE-1362095 (to T.V.R.) and the Center for Applied Plant Sciences (CAPS) at the Ohio State University (to T.V.R. and J.D.B.). Computational support from the Ohio Supercomputer Center is gratefully acknowledged.

REFERENCES

- Labinger, J. A.; Bercaw, J. E. *Nature* **2002**, *417*, 507.
- Rosenzweig, A. C. *Nature* **2015**, *518*, 309.
- Rolff, M.; Tuzek, F. *Angew. Chem., Int. Ed.* **2008**, *47*, 2344.
- Cramer, C. J.; Tolman, W. B. *Acc. Chem. Res.* **2007**, *40*, 601.
- Friedle, S.; Reisner, E.; Lippard, S. J. *Chem. Soc. Rev.* **2010**, *39*, 2768.
- Que, L., Jr.; Tolman, W. B. *Nature* **2008**, *455*, 333.
- Oloo, W. N.; Que, L., Jr. *Acc. Chem. Res.* **2015**, *48*, 2612.
- Chen, K.; Que, L., Jr. *J. Am. Chem. Soc.* **2001**, *123*, 6327.
- Thiabaud, G.; Guillemot, G.; Schmitz-Afonso, I.; Colasson, B.; Reinaud, O. *Angew. Chem., Int. Ed.* **2009**, *48*, 7383.
- Wei, N.; Murthy, N. N.; Chen, Q.; Zubieta, J.; Karlin, K. D. *Inorg. Chem.* **1994**, *33*, 1953.
- Gunsalus, N. J.; Konnick, M. M.; Hashiguchi, B. G.; Periana, R. A. *Isr. J. Chem.* **2014**, *54*, 1467.
- Kim, C.; Chen, K.; Kim, J.; Que, L., Jr. *J. Am. Chem. Soc.* **1997**, *119*, 5964.
- Maiti, D.; Lucas, H. R.; Narducci Sarjeant, A. A.; Karlin, K. D. *J. Am. Chem. Soc.* **2007**, *129*, 6998.
- Maiti, D.; Narducci Sarjeant, A. A.; Karlin, K. D. *J. Am. Chem. Soc.* **2007**, *129*, 6720.
- Tobey, S. L.; Jones, B. D.; Anslyn, E. V. *J. Am. Chem. Soc.* **2003**, *125*, 4026.
- Jo, H. H.; Lin, C.-Y.; Anslyn, E. V. *Acc. Chem. Res.* **2014**, *47*, 2212.
- You, L.; Berman, J. S.; Lucksanawichien, A.; Anslyn, E. V. *J. Am. Chem. Soc.* **2012**, *134*, 7126.
- You, L.; Pescitelli, G.; Anslyn, E. V.; Di Bari, L. *J. Am. Chem. Soc.* **2012**, *134*, 7117.
- Zhou, Y.; Yuan, Y.; You, L.; Anslyn, E. V. *Chem. - Eur. J.* **2015**, *21*, 8207.
- Joyce, L. A.; Maynor, M. S.; Dagna, J. M.; da Cruz, G. M.; Lynch, V. M.; Canary, J. W.; Anslyn, E. V. *J. Am. Chem. Soc.* **2011**, *133*, 13746.

- (21) Canary, J. W.; Allen, C. S.; Castagnetto, J. M.; Wang, Y. *J. Am. Chem. Soc.* **1995**, *117*, 8484.
- (22) Hermann, K.; Ruan, Y.; Hardin, A. M.; Hadad, C. M.; Badjic, J. D. *Chem. Soc. Rev.* **2015**, *44*, 500.
- (23) Liu, Z.; Tian, C.; Yu, J.; Li, Y.; Jiang, W.; Mao, C. *J. Am. Chem. Soc.* **2015**, *137*, 1730.
- (24) Rousseaux, S. A. L.; Gong, J. Q.; Haver, R.; Odell, B.; Claridge, T. D. W.; Herz, L. M.; Anderson, H. L. *J. Am. Chem. Soc.* **2015**, *137*, 12713.
- (25) Shook, R. L.; Borovik, A. S. *Inorg. Chem.* **2010**, *49*, 3646.
- (26) Izzet, G.; Zeng, X.; Akdas, H.; Marrot, J.; Reinaud, O. *Chem. Commun.* **2007**, 810.
- (27) Leenders, S. H. A. M.; Gramage-Doria, R.; de Bruin, B.; Reek, J. N. H. *Chem. Soc. Rev.* **2015**, *44*, 433.
- (28) Wittenberg, J. B.; Isaacs, L. *Supramol. Chem. Mol. Nanomater.* **2012**, *1*, 25.
- (29) Ruan, Y.; Dalkilic, E.; Peterson, P. W.; Pandit, A.; Dastan, A.; Brown, J. D.; Polen, S. M.; Hadad, C. M.; Badjic, J. D. *Chem. - Eur. J.* **2014**, *20*, 4251.
- (30) Oshovsky, G. V.; Reinhoudt, D. N.; Verboom, W. *Angew. Chem., Int. Ed.* **2007**, *46*, 2366.
- (31) Corbellini, F.; Di Costanzo, L.; Crego-Calama, M.; Geremia, S.; Reinhoudt, D. N. *J. Am. Chem. Soc.* **2003**, *125*, 9946.
- (32) Zadnard, R.; Junkers, M.; Schrader, T.; Grawe, T.; Kraft, A. *J. Org. Chem.* **2003**, *68*, 6511.
- (33) Rehm, T.; Schmuck, C. *Chem. Commun.* **2008**, 801.
- (34) Schmuck, C.; Schwegmann, M. *J. Am. Chem. Soc.* **2005**, *127*, 3373.
- (35) Canary, J. W.; Wang, Y.; Roy, R., Jr.; Que, L., Jr.; Miyake, H. *Inorg. Synth.* **1998**, *32*, 70.
- (36) Xiao, C.; Hao, F.; Qin, X.; Wang, Y.; Tang, H. *Analyst* **2009**, *134*, 916.
- (37) Quirt, A. R.; Lyyerla, J. R., Jr.; Peat, I. R.; Cohen, J. S.; Reynolds, W. F.; Freedman, M. H. *J. Am. Chem. Soc.* **1974**, *96*, 570.
- (38) Chen, S.; Ruan, Y.; Brown, J. D.; Gallucci, J.; Maslak, V.; Hadad, C. M.; Badjic, J. D. *J. Am. Chem. Soc.* **2013**, *135*, 14964.
- (39) Hirose, K. *Anal. Methods Supramol. Chem.* **2007**, 17.
- (40) Schneider, H. J., Duerr, H., Eds. *Frontiers in Supramolecular Organic Chemistry and Photochemistry*; VCH: Weinheim, 1991.
- (41) Badjic, J. D.; Nelson, A.; Cantrill, S. J.; Turnbull, W. B.; Stoddart, J. F. *Acc. Chem. Res.* **2005**, *38*, 723.
- (42) Cundari, T. R.; Deng, J. *J. Chem. Inf. Comput. Sci.* **1999**, *39*, 376.
- (43) You, L.; Anslyn, E. V. *Supramol. Chem. Mol. Nanomater.* **2012**, *1*, 135.
- (44) Ruan, Y.; Peterson, P. W.; Hadad, C. M.; Badjic, J. D. *Chem. Commun.* **2014**, *50*, 9086.
- (45) Voss, N. R.; Gerstein, M. *Nucleic Acids Res.* **2010**, *38*, W555.
- (46) Mecozzi, S.; Rebek, J., Jr. *Chem. - Eur. J.* **1998**, *4*, 1016.
- (47) Martin, N. H.; Allen, N. W.; Moore, J. C. *J. Mol. Graphics Modell.* **2000**, *18*, 242.
- (48) Schneider, H. J.; Schiestel, T.; Zimmermann, P. *J. Am. Chem. Soc.* **1992**, *114*, 7698.
- (49) Gibb, B. C. *Chemosensors* **2011**, 3.
- (50) Berova, N.; Di Bari, L.; Pescitelli, G. *Chem. Soc. Rev.* **2007**, *36*, 914.
- (51) Person, R.; Monde, K.; Humpf, H.-U.; Berova, N.; Nakanishi, K. *Chirality* **1995**, *7*, 128.
- (52) Stojanovic, S.; Turner, D. A.; Hadad, C. M.; Badjic, J. D. *Chem. Sci.* **2011**, *2*, 752.